Supplementary Information

Green, pliable Janus fabrics with efficient liquid management via needle punching, hydroentangling and wetting gradient

Author

Taotao Li[1], Heng Zhang[1*], Qi Zhen[2], Xiaoyu Guan[3], Qian Zhai[1], Ziqiang Yang[4]

1. College of Intelligent Textile and Textile Electronics, Zhongyuan University of Technology, No. 1 Huaihe Road, Xinzheng County, 451191, Zhengzhou, Henan Province, China.

2. College of Fashion Technology, Zhongyuan University of Technology, No. 1 Huaihe Road, Xinzheng County, 451191, Zhengzhou, Henan Province, China.

3. School of Materials Designing and Engineering, Beijing Institute of Fashion Technology, Beijing, 100029, China.

4. Henan Yeesain Health Technology Co., Ltd, Yuecun Town, Xinmi County, 452373 Zhengzhou, Henan Province, China.

*** Corresponding Author**

Heng Zhang, Ph.D.,

E-mail: zhangheng2699@zut.edu.cn, m-esp@163.com,

Tel: +86 156 3902 5712.

Address: College of intelligent textile and textile electronics, Zhongyuan University of Technology, No.1 Huaihe road, Xinzheng, Zhengzhou city, Henan province, China.

Supplementary Information

Figures

Figure S1 presents the tearing strength curves of the prepared Janus fabrics in the machine direction (MD) and cross direction (CD) under varying needling densities (*Nd*) and hydroentangling pressures (*Hp*). Specifically, **Figures S1a–b** illustrates the effect of *Nd* on tearing performance. As the *Nd* increased from 112 N/cm^2 to 392 N/cm^2, the peak tearing strength in the MD rose from 23.2 N to 43.8 N, and that in the CD increased from 4.8 N to 13.1 N, accompanied by a corresponding increase in tearing work. The marked difference in tearing strength between the MD and CD originates from the anisotropy in fiber orientation. In the MD, the POE/PP elastic filament web exhibit a pronounced preferential orientation; during tearing, these fibers are first stretched and elongated before yielding and fracturing, resulting in higher energy dissipation. In contrast, tearing in the CD occurs perpendicular to the fiber orientation, causing direct fiber fracture with lower force and tearing work. The monotonic increase in peak force with rising needle-punching density is attributed to the enhanced migration and greater embedding depth of Lyocell fibers into the POE/PP web per unit area, which generates more fiber entanglement points and substantially increases the degree of network entanglement.

Figures S1c–d depict the influence of *Hp* on tearing behavior. As the *Hp* increased from 100 bar to 150 bar, the peak force in the MD showed a slight increase from 26.2 N to 28.6 N, along with an increase in tearing work. Conversely, the peak force in the CD decreased markedly from 12.4 N to 5.0 N, accompanied by a reduction in tearing work. This opposite trend in tearing performance between the MD and CD is attributed to the orientation-selective fiber entanglement during hydroentangling. High-pressure water jets impinge on the fibrous web preferentially along the machine direction, promoting the entanglement and rearrange ment of loose fibers predominantly in the MD, thereby strengthening the MD fiber network. In contrast, the CD experiences a reduction in entangled fibers due to flow-induced fiber reorientation, which weakens its load-bearing capacity.

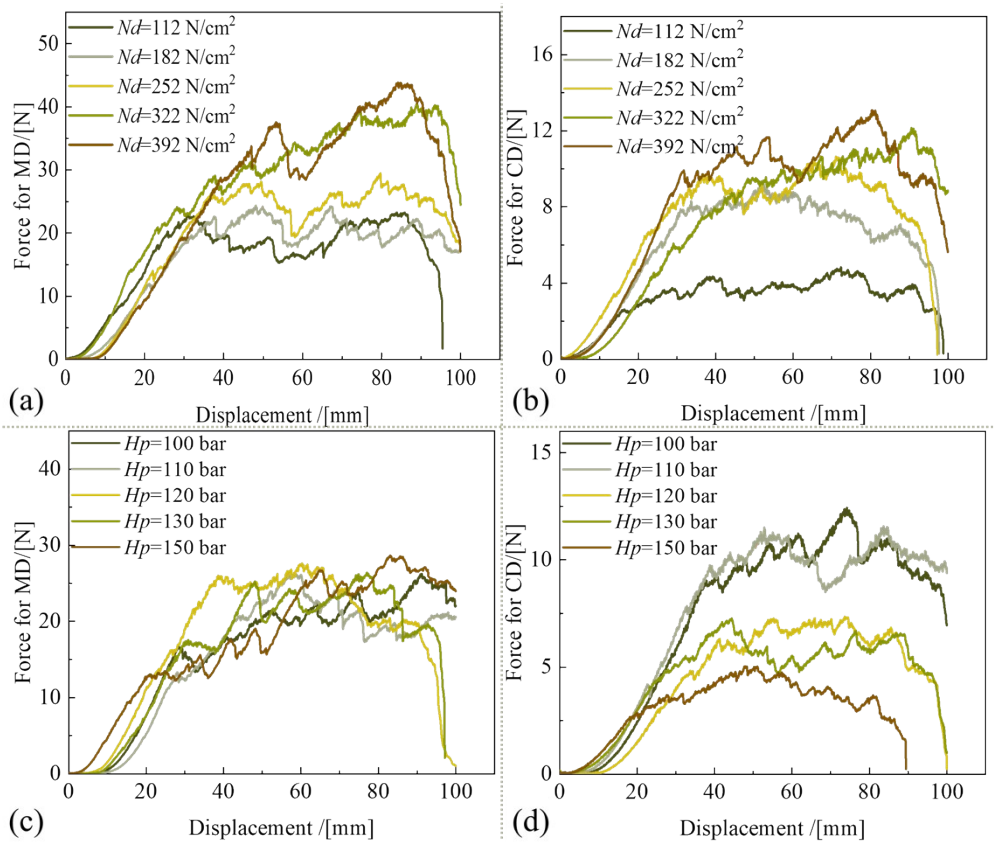

Figure S1. Force–displacement curves of tear strength tests along the (a) MD and (b) CD under different *Nd*, respectively. Force-displacement curves of tear strength tests along the (c) MD and (d) CD under different *Hp*, respectively.

Figure S2 presents the water vapor transmission rate (WVTR) of the prepared Janus fabrics under different *Nd* and *Hp*. As the *Nd* increased from 112 N/cm^2 to 392 N/cm^2, the WVTR decreased from 6242 g/(m^2·24h) to 6045 g/(m^2·24h). Similarly, when the *Hp* was raised from 100 bar to 150 bar, the WVTR declined from 6194 g/(m^2·24h) to 5923 g/(m^2·24h). These results indicate that WVTR decreases consistently with increasing *Nd* and *Hp*. This trend is attributed to the densification effect of both processes on the fibrous network. Higher *Nd* drives more Lyocell fibers to embed into the POE/PP elastic filament web, forming dense entanglement nodes and compressing the inter fiber pores. Increased *Hp*, through high-velocity water jets, further entangles and compacts the entire fiber web while refining the pore structure. Consequently, both the average pore size and the overall porosity of the fabric are significantly reduced. These structural evolutions collectively increase the tortuosity of the gas diffusion pathway, thereby diminishing the water vapor transmission capacity.

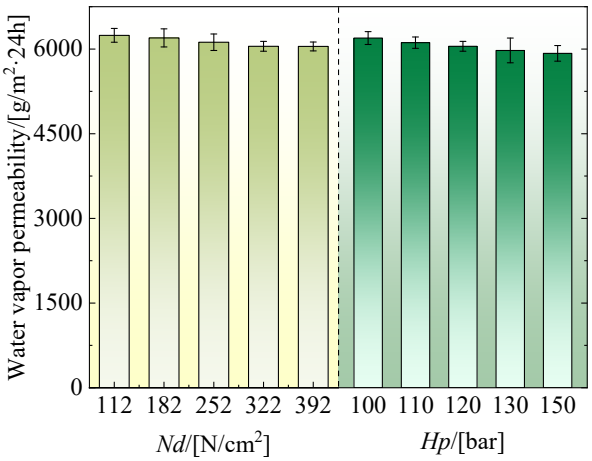

Figure S2. Water vapor permeability of the prepared Janus fabrics under different *Nd* and *Hp*

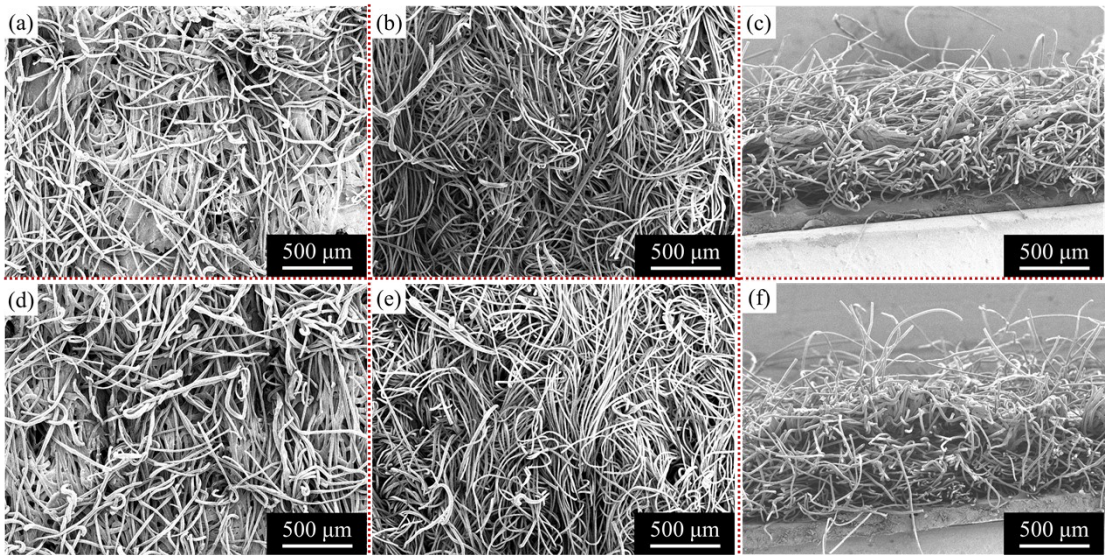

Figure S3. Surface electron microscopy image of POE/PP elastic filament web after (a) 5 washes and (d) 10 washes. Surface electron microscopy of Lyocell fibrous web after (b) 5 washes and (e) 10 washes. Cross-sectional electron microscope after (c) 5 washes and (f) 10 washes.

Figure S4 presents the relative accumulative one-way transport capacity (AOTC) of the Janus fabric after being stretched to fixed elongations of 20%, 30%, and 40% for 30 seconds, followed by relaxation to the original length. The AOTC was measured following the same MMT procedure described in the main text. As shown in **Figure S4**, the relative AOTC increased from 1229.7% at 20% strain to 1824.1% at 40% strain under the tested conditions. One possible explanation for this observation is that tensile stretching may partially align the fibrous structure and compress the through-thickness vertical channels formed by needle-punched Lyocell

fibers, which could potentially enhance the capillary pressure gradient and facilitate unidirectional liquid transport. However, it should be noted that the current experiment only examined the fabric after a single short-duration stretch, and the underlying mechanism requires further systematic investigation, including the effects of repeated stretching, different stretching rates, and potential structural changes such as pore size redistribution or fiber slippage.

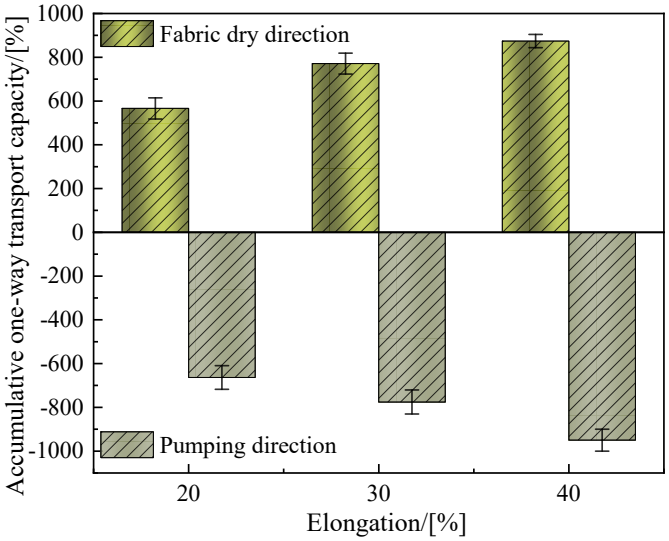

Figure S4. The AOTC of the Janus fabric after being stretched to fixed elongations of 20%, 30%, and 40% for 30 seconds

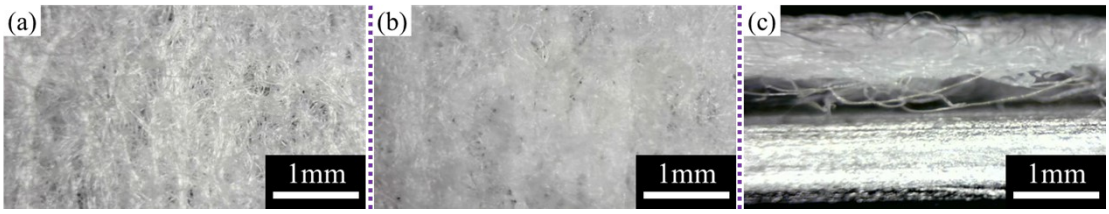

Figure S5. The stereo microscope images of the Janus fabric. Surface stereo microscopy image of Lyocell fibrous web (a). Surface stereo microscopy of POE/PP elastic filament web (b). Cross-sectional stereo microscope (c).

Supplementary Information

Tables

Table S1. The needle punching process parameters

Number	Needling frequency/[strokes/min]	Feed speed/[m/min]	*Nd*/[N/cm^2]
1	594	2.5	112
2		3.5	182
3		4.5	252
4		5.5	322
5		6.5	392

Table S2. The hydroentangling process parameters

Number	Width/[m]	Feed speed/[m/min]	*Hp*/[bar]
1	0.6	4.0	100
2			110
3			120
4			130
5			150

Table S3. Structural parameters of the prepared Janus fabrics under processed with varying *Nd* and *Hp*

Number	Technical parameters		Thickness/[mm]	Mass per unit area/[g/m^2]	Porosity/[%]
1	*Nd*/[N/cm^2]	112	0.516	107.1	84.29
2		182	0.530	109.5	84.35
3		252	0.535	108.4	84.65
4		322	0.533	105.6	84.99
5		392	0.544	107.6	85.02
6	*Hp*/[bar]	100	0.547	109.9	84.79
7		110	0.538	113.0	84.08
8		120	0.532	107.7	84.67
9		130	0.518	111.3	83.72
10		150	0.510	109.7	83.70

Table S4. Elastic recovery percentage and permanent deformation rate of the prepared Janus fabrics under different *Nd* and *Hp*

Number	Technical parameters		Elastic recovery percentage/[%]		Permanent deformation rate/[%]	
			MD	CD	MD	CD
1	*Nd*/[N/cm^2]	112	60.370	51.345	7.939	9.747
2		182	59.769	50.045	9.060	10.007
3		252	57.957	49.102	8.423	10.196
4		322	57.474	43.869	8.519	11.243
5		392	56.433	41.120	8.728	11.794
6	*Hp*/[bar]	100	61.457	57.717	7.721	8.469
7		110	60.502	55.505	7.913	8.912
8		120	60.323	54.846	7.949	9.044
9		130	57.322	57.787	8.538	9.056
10		150	57.168	52.085	8.582	9.598

Table.S5 The softness scores (W_a, W_b, W_c, W_d, W_e, P and S_1) of the prepared Janus fabrics under different *Nd* and *Hp*

Number	Technical parameters			W_a	W_b	W_c	W_d	W_e	P	S_1
1	Nd/ [N/cm^2]	MD	112	0.010	0.386	0.538	0.436	1.757	0.506	0.607
2			182	0.020	0.719	0.902	0.710	2.812	0.831	1.005
3			252	0.021	0.882	1.047	0.792	3.010	0.939	1.124
4			322	0.018	0.992	1.061	0.815	3.560	0.938	1.239
5			392	0.028	0.950	1.169	0.906	3.680	1.044	1.303
6		CD	112	0.009	0.138	0.159	0.110	0.648	0.136	0.200
7			182	0.023	0.253	0.252	0.159	0.760	0.203	0.277
8			252	0.005	0.249	0.276	0.194	0.790	0.225	0.293
9			322	0.011	0.184	0.286	0.219	0.904	0.255	0.310
10			392	0.001	0.235	0.314	0.219	0.963	0.255	0.332
11	Hp/ [bar]	MD	100	0.013	0.743	0.935	0.711	2.949	0.831	1.036
12			110	0.029	0.708	0.903	0.746	3.308	0.849	1.092
13			120	0.008	0.659	0.835	0.660	2.426	0.760	0.898
14			130	0.021	0.716	0.802	0.593	2.548	0.696	0.902
15			150	0.017	0.723	0.765	0.550	2.190	0.657	0.825
16		CD	100	0.008	0.135	0.190	0.119	0.803	0.156	0.234
17			110	0.006	0.165	0.229	0.151	0.772	0.201	0.254
18			120	0.016	0.170	0.255	0.155	0.893	0.215	0.284

19		130	0.013	0.156	0.215	0.149	0.822	0.194	0.258
20		150	0.001	0.116	0.191	0.131	0.715	0.171	0.220

Table S6. WT, AS, and SS on the UT and UB of the Janus fabrics under different *Nd* and *Hp*.

Number	Technical parameters		WT/[s]		AS/[%/s]		SS/[mm/s]	
			UT	UB	UT	UB	UT	UB
1	*Nd*/ [N/cm^2]	112	3.094	2.157	34.783	66.983	8.390	9.655
2		182	3.010	1.969	33.635	66.052	7.956	8.721
3		252	3.094	2.250	32.496	61.654	5.331	6.622
4		322	2.625	2.531	25.643	52.729	4.953	6.275
5		392	4.313	2.625	23.766	52.791	4.353	5.552
6	*Hp*/ [bar]	100	3.094	2.250	46.729	66.797	5.866	7.263
7		110	3.063	2.406	26.361	49.688	5.514	6.964
8		120	3.281	2.438	35.024	63.723	5.871	7.139
9		130	2.718	1.968	43.463	64.262	6.769	8.471
10		150	3.094	2.550	25.963	62.67	5.366	6.631

Table S7 Structural parameters of the prepared Janus fabrics under processed with different wash cycles

Number	Wash cycles	Thickness/[mm]	Mass per unit area/[g/m^2]	Porosity/[%]
1	5	0.579	115.9	84.84
2	10	0.557	114.8	84.37
3	20	0.540	112.4	84.22

Supplementary Information

Notes

Note S1 Estimation of capillary pressure difference between Lyocell and POE/PP layers

Based on the experimental data presented in the main text and the Supplementary Information, we have performed a quantitative estimation of this capillary pressure difference as follows.

1. Known parameters:

Surface tension of water: γ=0.072 N/m (at 25 °C);

Lyocell fibers: contact angle $\theta_L \approx 0°$, cos $\theta_L = 1$; average fiber diameter d_L=12.5 μm (**Figure 2h)**;

POE/PP fibers: contact angle $\theta_p \approx 120°$, cos $\theta_p = -0.5$; average fiber diameter d_p=20.1 μm (**Figure 2h)**;

Overall fabric porosity: from **Table S3** in the Supplementary Information, ε≈84%.

2. Estimation of the effective capillary radius

For a random fibrous network, the average pore diameter can be approximated by the following empirical relation:

$$d_{pore} \approx d_f \times \frac{1-\varepsilon}{\varepsilon}$$

Substituting the values:

For the Lyocell layer: $\frac{1-\varepsilon}{\varepsilon}$=0.16/0.84≈0.190, $d_{\text{pore, L}}$≈12.5×0.190≈2.38 μm, effective capillary radius $r_L=d_{\text{pore, L}}/2$≈1.19 μm.

For the POE/PP layer: similarly, $d_{\text{pore, P}}$≈20.1×0.190≈3.82 μm, r_P≈1.91 μm.

3. Capillary pressure calculation (Young-Laplace equation)

$$P_c = \frac{2\gamma\cos\theta}{r}$$

Lyocell fibrous web:

$$P_{c,L} = \frac{2\times 0.072\times 1}{1.19\times 10^{-6}} = \frac{0.144}{1.19\times 10^{-6}} \approx 121\text{kPa}$$

POE/PP fibrous web:

$$\boldsymbol{P}_{\boldsymbol{c},\boldsymbol{P}} = \frac{2 \times 0.072 \times (-0.5)}{1.91 \times 10^{-6}} = \frac{-0.072}{1.91 \times 10^{-6}} \approx -37.7\text{kPa}$$

Capillary pressure difference:

$$\Delta \boldsymbol{P} = \boldsymbol{P}_{\boldsymbol{c},\boldsymbol{L}} - \boldsymbol{P}_{\boldsymbol{c},\boldsymbol{P}} \approx 121 - (-37.7) = 158.7\text{kPa}$$